HHS Public Access

Author manuscript

Mol Cell Endocrinol. Author manuscript; available in PMC 2023 April 15.

Published in final edited form as:

Mol Cell Endocrinol. 2022 April 15; 546: 111577. doi:10.1016/j.mce.2022.111577.

Deletion of the homeodomain gene *Six*3 from kisspeptin neurons causes subfertility in female mice

Shanna N. Lavalle, **Teresa Chou**, **Jacqueline Hernandez**, **Nay Chi P. Naing**, **Michelle Y. He**, **Karen J. Tonsfeldt**, **Pamela L. Mellon***

Department of Obstetrics, Gynecology, And Reproductive Sciences, Center for Reproductive Science and Medicine, University of California, San Diego, La Jolla, CA, 92093, USA

Abstract

The homeodomain transcription factor SIX3 is a known regulator of eye, nose, and forebrain development, and has recently been implicated in female reproduction. Germline heterozygosity of SIX3 is sufficient to cause subfertility, but the cell populations that mediate this role are unknown. The neuropeptide kisspeptin is a critical component of the reproductive axis and plays roles in sexual maturation, ovulation, and the maintenance of gonadotropin secretion. We used Cre-Lox technology to remove *Six3* specifically from kisspeptin neurons in mice to test the hypothesis that SIX3 in kisspeptin neurons is required for reproduction. We found that loss of *Six3* in kisspeptin neurons causes subfertility and estrous cycle irregularities in females, but no effect in males. Overall, we find that SIX3 expression in kisspeptin neurons is an important contributor to female fertility.

Keywords

Six3; Fertility; Kisspeptin; Cre/LoxP; Hypothalamus

1. Introduction

Activation and maintenance of the hypothalamic-pituitary-gonadal (HPG) axis is necessary for the transition from adolescence to adulthood and reproductive competence. Dysregulation along the HPG axis can lead to reduced or complete loss of fertility. Idiopathic hypogonadotropic hypogonadism (IHH) and its anosmic counterpart, Kallmann

*Corresponding author. University of California, San Diego 9500 Gilman Drive, La Jolla, CA, USA, 92093, pmellon@health.ucsd.edu (P.L. Mellon).

Declaration of competing interest

Authors have no conflict of interest.

CRediT authorship contribution statement

Shanna N. Lavalle: Conceptualization, Methodology, Validation, Formal analysis, Investigation, Data curation, Writing – original draft, Writing – review & editing, Visualization. **Teresa Chou:** Validation, Formal analysis, Investigation, Writing – review & editing. **Jacqueline Hernandez:** Validation, Investigation, Writing – original draft, Writing – review & editing. **Nay Chi P. Naing:** Validation, Investigation, Writing – review & editing. **Michelle Y. He:** Validation, Investigation, Writing – review & editing. **Karen J. Tonsfeldt:** Methodology, Validation, Data curation, Investigation, Writing – review & editing, Visualization. **Pamela L. Mellon:** Conceptualization, Methodology, Validation, Formal analysis, Resources, Data curation, Writing – review & editing, Visualization, Supervision, Project administration, Funding acquisition.

syndrome, are examples of reproductive disorders that lead to delayed or absent puberty. IHH is a genetic disorder characterized by insufficient production or secretion of gonadotropin-releasing hormone (GnRH), leading to reduced sex steroid production and hypogonadism (Au et al., 2011; Bianco and Kaiser, 2009; Topaloglu, 2017). In humans, approximately 5% of normosmic IHH cases are attributed to genetic disruptions of kisspeptin signaling (Bianco and Kaiser, 2009).

The neuropeptide kisspeptin has established roles in puberty, ovulation, and maintenance of pulsatile GnRH and resulting luteinizing hormone (LH) and follicle-stimulating hormone (FSH) secretion (Gottsch et al., 2004; Kauffman, 2010; Messager et al., 2005). *Kiss1* is differentially regulated in the arcuate nucleus (ARC) and the anteroventral periventricular nucleus (AVPV), leading to differing roles in reproduction (Smith et al., 2005a, 2005b). ARC kisspeptin neurons are considered important for the pulse generator and mediate sex steroid negative feedback, leading to reduced *Kiss1* expression in the presence of androgens and estrogens (Herbison, 2018; McQuillan et al., 2019; Smith et al., 2005b). AVPV kisspeptin neurons are sexually dimorphic and primarily occur in females, where they mediate the circadian-gated, estradiol (E2)-induced LH surge and induce *Kiss1* expression in the presence of E2 (Dror et al., 2013; Dungan et al., 2007; Smith et al., 2005a, 2006).

Recent studies in mice have implicated homeodomain transcription factors, such as VAX1 and SIX3, as potential IHH gene candidates (Hoffmann et al., 2014, 2019; Pandolfi et al., 2018). In mice, deletion of *Vax1* from GnRH neurons results in infertility (Hoffmann et al., 2016), whereas deletion of *Vax1* from kisspeptin neurons alters *Kiss1* gene expression but does not impact fertility (Lavalle et al., 2021). *Six3*, which plays a critical role in eye, nose, and forebrain development (Conte et al., 2005; Lagutin et al., 2003), is also critical to reproduction in mice. The loss of a single allele results in strong reproductive defects, many of which recapitulate those seen in patients with IHH and Kallmann syndrome, including reduced GnRH neurons in the hypothalamus, altered estrous cyclicity, subfertility, and anosmia (Pandolfi et al., 2018). However, heterozygous $Six3^{+/-}$ mice maintain approximately 55% of GnRH neurons in the hypothalamus during adulthood, which is sufficient to maintain reproductive function in female mice (Herbison et al., 2008). Furthermore, conditional deletion of *Six3* specifically from GnRH neurons did not recapitulate any of the phenotypes seen in the heterozygous $Six3^{+/-}$ mice, and there were no impairments to fertility, suggesting that SIX3 in reproduction occurs in cell populations outside of GnRH neurons (Pandolfi et al., 2018).

In our current study, we tested the hypothesis that SIX3 in kisspeptin neurons is necessary for fertility by specifically deleting *Six3* from *Kiss1*-expressing cells. We found that SIX3 within kisspeptin neurons is necessary for female fertility, but not male, and may play a role in the timing of LH release in the presence of E2.

2. Materials and methods

2.1. Animals

All animal procedures were performed in accordance with the University of California San Diego, Institutional Animal Care and Use Committee regulations. To delete *Six3*

from *Kiss1*-expressing cells, we crossed $Six3^{flox/flox}$ mice (RRID:MGI:3693848) (Liu et al., 2006) with $Kiss1^{Cre}$ mice (RRID:IMSR_JAX:023,426) (Cravo et al., 2011) to generate $Six3^{Flox/Flox}$:$Kiss1^{Cre}$ mice ($Six3^{KissCre}$) and $Six3^{flox/flox}$:$Kiss1^{WT}$ mice ($Six3^{flox/flox}$). We used Ai14 Rosa-tdTomato mice (RRID: IMSR_JAX:007914) (Madisen et al., 2010) to create a Kiss1 reporter line by crossing them to $Kiss1^{Cre}$ mice to generate $Kiss1^{Cre}$:tdTomato mice. All mice were on a mixed NMRI and C57/Bl6 background. Mice were group housed and maintained on a 12-h light, 12-h dark cycle with *ad libitum* chow and water.

Genotyping of the mice was performed by PCR with genomic DNA collected from tail tips. *Six3* wildtype (WT) and *Six3* flox alleles were detected using Six3-For: 5′-CCCCTAGCCTAACCCAAACAT-3′ and Six3-Rev: 5′-CGGCCCATGTACAACGCGTAT-3′ primers. Germline recombination was detected using Six3-For and Six3-Rec-Rev: 5′-TTCCCCTCTTTGACTCCTATG-3′ primers. Cre-For: 5′-GCATTACCGGTCGTAGCAACGAGTG-3′ and Cre-Rev: 5′-GAACGCTAGAGCCTGTTTTGCACGTTC-3′ primers were used to detect the Cre allele. tdTomato was detected using tdtF1: 5′-GGCATTAAAGCAGCGTATCC-3′, tdtR1 5′-CTGTTCCTGTACGGCATGG-3, tdtF2: 5′-CCGAAAATCTGTGGGAAGTC-3′, and tdtR2: 5′-AAGGGAGCTGCAGTGGAGTA-3. Mice that were positive for *Six3* germline recombination in tail samples or exceeded 60 g in body weight were removed from the study.

2.2. Fluorescent in-situ hybridization

20 μm serial coronal sections were collected from fresh frozen brains, spanning the length of the AVPV, ARC, and reticular thalamic nucleus (Di Giorgio et al., 2013; Sunnen et al., 2014; Tonsfeldt et al., 2019). AVPV sections were collected from ovariectomized (OVX)+E2 treated females. ARC and reticular thalamic nucleus sections were collected from OVX females. Sections were mounted on Superfrost Plus Microscope Slides (Fisher Scientific) and stored at −80 °C until further processing. Slides were fixed in chilled 4% PFA, washed two times with 1X PBS, and dehydrated in ethanol. Probes to detect *Kiss1* (500,141), *cFos* (316,921-C2), and *Six3* (855,211-C3) were used with the highly sensitive RNAscope Multiplex Fluorescent v2 Assay (Advanced Cell Diagnostic, 323,100), according to manufacturer's instructions. Sections were counterstained with DAPI and coverslipped with ProLong Gold (Invitrogen). All AVPV slides were processed in a single assay and all ARC and reticular thalamic nucleus slides were processed in a single assay.

2.3. Microscopy and analysis

Fluorescent microscopy was performed at the Nikon Imaging Core (UCSD) using a Nikon Eclipse Ti2-E microscope with Plan Apo objectives. Samples were excited by the Lumencor SpectraX and acquired with a DS-Qi2 CMOS camera using NIS-Elements software, or with a laser scanning confocal (A1R HD, Nikon), acquired with an iXon Ultra 897 EMCCD camera (Andor). All AVPV slides were imaged at the same time and under the same conditions. All ARC and thalamic reticular nucleus slides were imaged at the same time and under the same conditions. The number of *Kiss1* cells that colocalized with *Six3* or atypical signal was determined manually, using FIJI Cell Counter tool. NIS-Elements: General Analysis software was used to objectively quantify the intensity of *Kiss1, cFos,*

and *Six3* signals. A signal threshold of 2.5 standard deviations above background was used for defining positive signal of each gene. *cFos* and *Six3* signals were quantified only in *Kiss1*-positive cells.

2.4. Fertility and plugging assessment

To assess fertility in females, 15–18-week-old virgin $Six3^{flox/flox}$ or $Six3^{KissCre}$ females were paired with a virgin wildtype male for 90 days. The number of litters and the number of pups in each litter were recorded. Fertility of the wildtype males of the infertile pairs were not further assessed due to the age at disbanding. To assess male mating behavior and fertility, 10–16-week-old virgin $Six3^{flox/flox}$ or $Six3^{KissCre}$ males were paired with a wildtype female for 60 days. For the first 10 days, females were checked for the presence of plugs. The number of pups produced from each litter were recorded.

2.5. Ovarian histology

Following the fertility assay, female mice were separated from males and provided time to birth their final litters, then ovaries were collected during diestrus. Upon dissection, ovaries were placed in a solution of 60% EtOH, 30% formaldehyde, and 10% glacial acetic acid. Fixed ovaries were paraffin embedded, serial sectioned at 12 μm on a microtome, and stained with hematoxylin and eosin (H&E; Sigma-Aldrich). The number of Graafian follicles, identified by the presence of large antral space surrounding the oocyte, and the number of corpora lutea within a single ovary was quantified independently by two individuals, blinded to genotype. Every fifth section was scored to ensure follicles and corpora lutea were not double counted.

2.6. Pubertal onset and estrous cyclicity

After weaning, mice were checked daily for vaginal opening in females and preputial separation in males to determine pubertal onset (Hoffmann, 2018). In females, vaginal smears were taken daily from pubertal onset until first estrus or when they reached 90 days of age. To assess estrous cyclicity, vaginal smears were taken for 16 consecutive days from 12-week-old females. Vaginal smears were stained with 0.1% methylene blue, and a single observer, blinded to genotype, determined stage of cell cycle based on the composition of cell types present (Byers et al., 2012).

2.7. Hormone analysis

For diestrus-staged female mice, blood was collected from tail vein via capillary tube (Drummond microcaps 40 μL), sealed with Critoseal, allowed to clot at room temperature for 1 h, centrifuged at 2000×*g* for 15 min, and then serum was collected and stored at −20 °C until assayed on Luminex Magpix. Serum LH and FSH were measured by Luminex assay according to manufacturer's instructions (LH: lower detection limit, 4.92 pg/mL; intra-assay CV, <14.10%; inter-assay CV 7.28%; FSH: lower detection limit, 9.5 pg/mL; intra-assay CV, 12.13% inter-assay CV 7.22%). For OVX + E2-treated females and intact males, blood samples were collected at time of euthanasia, allowed to clot at room temperature for 1 h, centrifuged at 2000×*g* for 15 min, and then serum was collected and stored at −20 °C until assayed for LH and FSH by The University of Virginia Center

for Research in Reproduction Ligand Assay and Analysis Core. LH was measured using LH RIA with a reportable range between 0.02 and 75.0 ng/mL (intra-assay CV = 5.5%, inter-assay CV = 8.4%). FSH was measured using FSH RIA with a reportable range between 3.0 and 75.0 ng/mL (intra-assay CV = 7.5%, inter-assay CV = 10.1%).

2.8. Luteinizing hormone (LH) surge

12–16-week-old virgin female mice weighing between 18 and 28 g were ovariectomized between zeitgeiber time (ZT) 2–5. A pellet containing 0.75 μg of 17-β estradiol dissolved in sesame oil was implanted subcutaneously to mimic proestrus levels of E2 (Dror et al., 2013). Two days after surgery, mice were sacrificed either in the morning (AM), between ZT 4–5, or at the time of lights off (PM), between ZT 12–13. Serum and brains were collected at sacrifice. An LH surge was conservatively defined as LH values that were three standard deviations above the AM average (Dungan et al., 2007). AM values plus 3 standard deviations amounted to: 0.65 for $Six3^{Flox/Flox}$, 0.90 for $Six3^{KissCre}$, and 0.92 when values for $Six3^{Flox/Flox}$ and $Six3^{KissCre}$ were combined. We used the most stringent value of 0.92 for defining a surge in all mice.

2.9. Cell culture

KTaR-1 (RRID:CVCL_VS93) and KTaV-3 (RRID:CVCL_VS94) immortalized kisspeptin cell lines (Jacobs et al., 2016) were kindly provided by Dr. Patrick Chappell (Oregon State University). Cells were maintained in complete media consisting of DMEM (Corning) with 10% fetal bovine serum (FBS) (Omega Scientific) and 1% penicillin-streptomycin (HyClone) and incubated at 37°C with 5% CO_2.

2.10. Plasmids

The −1313/+26 human *KISS1*-pGL2-luciferase plasmid (hKiss-Luc) (Mueller et al., 2011) was kindly provided by Alejandro Lomniczi and Sergio Ojeda. The −4058/+455 mouse *Kiss1*-pGL4-luciferase plasmid (Atkin et al., 2013) was kindly provided by Dr. Steven Kliewer (UT Southwestern). We subcloned the −4058/+455 mouse *Kiss1* promoter sequence from the pGL4 backbone into a pGL2 backbone using the *Kpn*I-HF, *Xho*I, and *Sal*I-HF restriction enzymes in 10X Cut Smart Buffer (New England BioLabs) and religated using Quick Ligase Kit (New England BioLabs). This resulted in the −4058/+455 mouse Kiss1-Luciferase-pGL2 plasmid (mKiss-Luc). The murine −1 kb cFos-pGL3-Luciferase (cFos-Luc) (Ely et al., 2011) and the cFos-Luc with cis-mutations at −59 (μ−59), −313 (μ−313), and at both −59 and −313 (μ−313x-59) bp were previously described (Hoffmann et al., 2018). The reporter plasmid containing β-galactosidase constitutively driven by the Herpes virus thymidine kinase promoter (TK-βgal) was used to control for transfection efficiency. We obtained the SIX3-pSG5 expression plasmid from Origene Technologies (Rockville, MD) and the murine cFOS-CMV expression plasmid (cFOS) was previously described (Glidewell-Kenney et al., 2013). Sequences of all plasmids were confirmed by Sanger Sequencing (Eton Bioscience).

2.11. Transient transfections and luciferase assays

One day prior to transient transfections, KTaR-1 or KTaV-3 cells were seeded at 30×10^4 cells per well in 12-well plates with complete media and allowed to grow overnight. Transient transfections were performed using Polyjet In Vitro DNA Transfection Reagent (SignaGen Laboratories), following manufacturer's instructions. Cells were transfected with 500 ng of reporter plasmid (hKiss-Luc, mKiss-Luc, cFos-Luc, μ−313, μ−59, μ−313x-59) or backbone (pGL2 or pGL3), and co-transfected with 100 ng of TK-βgal and 20 ng SIX3 expression vector or pSG5-empty vector (EV) or 50 ng cFOS expression vector or CMV-empty vector (EV). Polyjet/DNA was removed 24 h after transfection treatment and replaced with complete medium. 48 h from start of transfection, cells were harvested for luciferase assay. To harvest cells, medium was aspirated from wells, cells were washed with 1X PBS, and then lysed with 0.1 M K-phosphate buffer, pH 7.8, containing 0.2% Triton X-100. Luciferase and β-galactosidase assays were performed as previously described. All conditions were performed in triplicate. Within each well, luciferase values were normalized to TK-βgal values, then triplicate luciferase/TK-βgal values were averaged. hKiss-Luc and mKiss-Luc values were normalized to pGL2 and cFos-Luc, μ−313, μ−59, and μ−313x-59 values were normalized to pGL3.

2.12. Statistical analysis

Differences between groups were detected by Student's t-test, Welch's *t*-test, one-way ANOVA, or two-way ANOVA using Prism 9 (Graphpad). For one-way and two-way ANOVA, significant effects were followed by Tukey's Honest Significant Difference test. Residuals were checked for normality using Shapiro Wilk test ($p < 0.05$). When needed, data were log transformed and reanalyzed, where indicated.

3. Results

3.1. Loss of SIX3 from Kiss1-expressing cells reduces fecundity in female mice

To test the hypothesis that SIX3 within kisspeptin neurons regulates reproduction, we specifically deleted *Six3* from *Kiss1* cells by crossing $Six3^{Flox/Flox}$ mice to $Kiss1^{Cre}$ mice to generate $Six3^{Flox/Flox}$:$Kiss1^{Cre}$ mice ($Six3^{KissCre}$) and $Six3^{Flox/Flox}$:$Kiss1^{WT}$ mice ($Six3^{F/F}$). Exon 1 of the *Six3* allele, which contains both the *Six* domain and the homeodomain, is flanked by LoxP sites, allowing this region to be excised from *Kiss1* cells in $Six3^{KissCre}$ mice and remain intact in $Six3^{Flox/Flox}$ mice (Fig. 1A). We used fluorescent *in situ* hybridization to assess knockdown efficiency in the AVPV of $Six3^{Flox/Flox}$ and $Six3^{KissCre}$ mice using a *Six3* probe that spans the 5' UTR and Exon 1 of the *Six3* gene (Fig. 1A and B). We found that 46.7% of AVPV kisspeptin neurons colocalized with *Six3* in $Six3^{Flox/Flox}$ mice compared to 6.7% in $Six3^{KissCre}$ mice (Fig. 1C). We also found that *Six3* is expressed in 20.7% of *Kiss1*-positive cells in the ARC of $Six3^{Flox/Flox}$ mice and is reduced to 2.8% in $Six3^{KissCre}$ mice (Fig. 1D and E). We observed distinct punctate *Six3* signal in both *Kiss1*-negative and *Kiss1*-positive cells in $Six3^{Flox/Flox}$ mice (Fig. 1D and E). In $Six3^{KissCre}$ mice, 50.6% of AVPV *Kiss1* cells and 43.5% of ARC *Kiss1* cells displayed atypical, large, and circular fluorescent signal, potentially an artifact left from the excision by Kiss1-Cre (Fig. 1B, D). $Six3^{KissCre}$ mice maintained the clear punctate signal in *Kiss1*-negative cells in the AVPV, ARC, and reticular thalamic nucleus, a region reported to have high *Six3* expression

levels (Conte et al., 2005; Sunnen et al., 2014), demonstrating nearby cell populations retain intact *Six3* and that the atypical signal is not representative of high *Six3* expression (Fig. 1B, D, F). We did observe atypical signal in a subset of cells that did not express *Kiss1* mRNA in the AVPV and ARC of $Six3^{KissCre}$ mice. This may be due to cells that previously expressed *Kiss1* but were no longer expressing *Kiss1* mRNA, as there are more cells labeled with tdTomato in a Kiss1-tdTomato reporter mouse than detectable *Kiss1* mRNA in the AVPV of an OVX + E2 treated $Six3^{Flox/Flox}$ mouse (Fig. 1G), because tdTomato reporter records cells that have expressed Kiss-cre at any time throughout development or because *Kiss1* levels are below detection in some of the cells while the tdTomato signal is more robust and not regulated by steroid hormones.

To assess the role of kisspeptin cell specific SIX3 in reproduction, we paired $Six3^{Flox/Flox}$ and $Six3^{KissCre}$ females with a wildtype male for 90 days. We found that there were no significant differences in the number of days to produce their first litter (Fig. 2A), or in the total number of litters produced. However, a subset of $Six3^{KissCre}$ mice did not produce a single litter within the 90 days (Fig. 2A and B). We also examined litter size and found that the fertile $Six3^{KissCre}$ females had significantly fewer pups per litter compared to $Six3^{Flox/Flox}$ females (Fig. 2C). To determine if the reduced fecundity was due to an ovulatory defect, we assessed ovarian morphology (Fig. 2D). $Six3^{KissCre}$ females had a significant reduction in the number of Graafian follicles compared to $Six3^{Flox/Flox}$ females (Fig. 2E), and, while there appeared to be a reduction in the number of corpora lutea in $Six3^{KissCre}$ mice (Fig. 2F), the difference was not significant. In contrast to females, male $Six3^{KissCre}$ mice had no impairments to fertility as they were able to plug wildtype female mice in a similar time frame as $Six3^{Flox/Flox}$ males (Fig. 2G) and produced a similar number of pups per litter (Fig. 2H). Because the loss of *Six3* from kisspeptin neurons had no effect on male fertility, we focused the remainder of the study on female $Six3^{KissCre}$ mice.

3.2. Loss of SIX3 in kisspeptin cells disrupts female estrous cycles

We next determined whether sexual maturation was affected by the loss of SIX3 from kisspeptin neurons in female mice. We found that the loss of *Six3* did not alter the time to pubertal onset, as indicated by vaginal opening (Fig. 3A) or the weight at vaginal opening (Fig. 3B). The time to reach first estrus, another marker of sexual maturation, was also unaffected (Fig. 3C). Female mice have a four to five day estrous cycle in which they transition from diestrus to proestrus and then estrus (Byers et al., 2012), as shown in representative images of our $Six3^{Flox/Flox}$ females (Fig. 3D). $Six3^{KissCre}$ females, however, had impaired estrous cycles (Fig. 3E). $Six3^{KissCre}$ females spent significantly more time in diestrus and a significantly less time in estrus (Fig. 3F) and took approximately twice as long to complete a full cycle (diestrus to diestrus; Fig. 3G) compared to $Six3^{Flox/Flox}$ females.

3.3. $Six3^{KissCre}$ females have elevated LH levels during the morning of induced LH surge

Circulating FSH and LH were similar between diestrus $Six3^{Flox/Flox}$ and $Six3^{KissCre}$ females when collected between ZT 4–6 (Fig. 4A and B). Because some of the $Six3^{KissCre}$ mice did not produce any litters during the fertility assay, we performed an induced LH surge paradigm (OVX + E2) and found that 7 of 9 $Six3^{KissCre}$ females were able to induce an LH surge, as well as 5 of 5 $Six3^{Flox/Flox}$ mice (Fig. 4C). Interestingly, AM $Six3^{KissCre}$

females had significantly elevated levels of LH compared to AM $Six3^{Flox/Flox}$ mice (Fig. 4C); however, 7 of 9 $Six3^{KissCre}$ mice still had PM LH levels more than three times the standard deviation of the AM $Six3^{KissCre}$ levels.

To understand what might be driving the elevated AM LH levels in $Six3^{KissCre}$ mice, we collected brains from both AM and PM $Six3^{Flox/Flox}$ and $Six3^{KissCre}$ OVX + E2-treated females and visualized AVPV *Kiss1* and *cFos* expression by *in situ* hybridization (Fig. 5A). The intensity of *Kiss1* was significantly higher in the PM groups compared to the AM groups (Two-way ANOVA, $p < 0.0001$). The loss of SIX3 from $Six3^{KissCre}$ mice did not alter the number of *Kiss1*-expressing cells (Fig. 5B) or the intensity of the *Kiss1* signal in the AVPV of AM or PM females (Fig. 5C). There were no differences in ARC *Kiss1* intensity between $Six3^{Flox/Flox}$ and $Six3^{KissCre}$ OVX + E2-treated females at either the AM or PM time points (AM $Six3^{Flox/Flox} = 0.235 \pm 0.054$, AM $Six3^{KissCre} = 0.192 \pm 0.049$, PM $Six3^{Flox/Flox} = 0.145 \pm 0.066$, PM $Six3^{KissCre} = 0.135 \pm 0.012$, N = 3–4). The percent of *Kiss1* cells colocalized with *cFos* was significantly higher in the PM group compared to the AM group (Two-way ANOVA, $p < 0.05$) and there was a significant reduction in the percent colocalization in AM $Six3^{KissCre}$ mice compared to AM $Six3^{Flox/Flox}$ mice (Fig. 5D). Consistent with our LH findings, the intensity of *cFos* was significantly increased in AM $Six3^{KissCre}$ mice compared to AM $Six3^{Flox/Flox}$ mice; however, no difference was observed in *cFos* intensity between PM $Six3^{Flox/Flox}$ and PM $Six3^{KissCre}$ mice (Fig. 5E).

3.4. Six3 expression in AVPV kisspeptin neurons is regulated by time of day

Because we only observed changes in *cFos* colocalization and expression in OVX + E2-treated mice in the AM, we investigated whether *Six3* expression levels were affected by time of day. We used fluorescent *in situ* hybridization to assess *Six3* expression patterns in the AVPV of $Six3^{Flox/Flox}$ OVX + E2-treated females (Fig. 6A). We found that there was no significant difference in the percentage of *Kiss1* cells that colocalized with *Six3* between the AM and PM timepoints (Fig. 6B). However, we did observe that *Six3* intensity was significantly lower in the evening (PM), when the LH surge is expected to occur, than in the morning (AM) (Fig. 6C), indicating that *Six3* expression in AVPV kisspeptin neurons is regulated by time of day.

3.5. SIX3 represses cFos-Luc transcription *in vitro*

While the loss of SIX3 from AVPV kisspeptin cells did not alter *Kiss1* mRNA *in vivo*, we next tested whether overexpression of SIX3 could modulate *Kiss1* transcription *in vitro*. We used immortalized kisspeptin cell lines derived from the AVPV (KTaV-3) or ARC (KTaR-1) of a female mouse hypothalamus (Jacobs et al., 2016) and cotransfected a human *Kiss1* luciferase (hKiss-Luc) or mouse *Kiss1* luciferase (mKiss-Luc) reporter plasmid with a SIX3 expression vector. We found that overexpression of SIX3 significantly repressed hKiss-Luc transcription in both KTaV-3 (Fig. 7A) and KTaR-1 (Fig. 7B) cells but did not alter mKiss-Luc transcription in either cell line (Fig. 7C and D). Because we observed altered *cFos* expression in AVPV kisspeptin cells in the morning of an induced LH surge, we determined whether SIX3 could regulate transcription of *cFos*, which has one complete ATTA and a partial (ATTxA) SIX3 binding site located −313 and −59 base pairs upstream of the proximal promoter, respectively (Fig. 6E). Using a murine −1 Kb *cFos*-luciferase

(cFos-Luc), we demonstrate that SIX3 can act as a repressor of *cFos*-Luc transcription in KTaV-3 cells (Fig. 7F). We then tested whether the repression by SIX3 was being mediated through either of the 2 sites. We found that loss of a single ATTA or ATTxA site was not sufficient to prevent SIX3 induced repression of the *cFos* promoters. However, SIX3 could no longer repress cFos-Luc transcription when both sites were mutated (Fig. 7G). We were also interested in whether cFOS could act as a transcription factor to regulate the *Kiss1* promoter which contains an AP-1 consensus sequence, a potential binding site for cFOS. We found that overexpression of cFOS significantly induced mKiss-Luc transcription (Fig. 7H).

4. Discussion

Heterozygous loss of the homeodomain transcription factor, *Six3*, has previously been shown to cause subfertility in mice (Hoffmann et al., 2019; Pandolfi et al., 2018); while *Six3* is expressed in several areas of the adult brain and pituitary, the specific cell types that mediate this effect are unknown. *Six3* heterozygous mice have functional pituitaries, normal ovarian and testicular morphology, and the homozygous loss of *Six3* from GnRH neurons produced no reproductive impairments (Pandolfi et al., 2018). We therefore decided to examine the role of *Six3* in kisspeptin neurons, which act upstream of GnRH neurons. We found that the loss of *Six3* in kisspeptin neurons shared some features of subfertility and disrupted estrous cyclicity seen in the *Six3* heterozygous mice, indicating that the heterozygous phenotype is mediated at least in part by loss of *Six3* in kisspeptin neurons.

We confirm that *Six3* is expressed in approximately half of AVPV and 20% of ARC kisspeptin neurons in adult $Six3^{Flox/Flox}$ mice, and that kisspeptin-specific *Six3* expression is disrupted in $Six3^{KissCre}$ mice, leading to reduced fertility. Although we observed an atypical fluorescent signal in *Kiss1*-positive cells in $Six3^{KissCre}$ mice, we do not believe this signal represents functional *Six3* mRNA that is being translated to SIX3 protein. If a truncated protein were made containing exon 2, it would not contain the functional Six domain or homeodomain and would not be detected by the *Six3* probe that targets exon 1. It is likely an artifact produced by the recombination as we do not see this atypical signal in regions that express *Six3* but do not express Kiss1-Cre, such as the reticular thalamic nucleus. Conditional deletion of *Six3* using the Six3-flox mouse has been used by others to demonstrate developmental, reproductive, and circadian phenotypes in mice (Hoffmann et al., 2021; Liu et al., 2006; Pandolfi et al., 2018). The $Kiss1^{Cre}$ mouse is well characterized and has been used by many in the field to efficiently delete genes specifically in kisspeptin neurons (Cravo et al., 2011; Ho et al., 2021; Stephens et al., 2015). If *Six3* remained functional, we would not see the reproductive phenotypes that were observed in the $Six3^{KissCre}$ mice.

We found that the loss of *Six3* from kisspeptin neurons resulted in a subset of $Six3^{KissCre}$ females being unable to produce a single litter within a 90-day fertility assay. Furthermore, the $Six3^{KissCre}$ females that were able to produce litters had reduced fecundity compared to $Six3^{Flox/Flox}$ females, which was a more robust reproductive effect compared to *Six3* heterozygous females who had a delay to first litter, but normal fecundity (Pandolfi et al., 2018). The decreased fecundity is likely due to an impairment in follicular maturation or survival as there were significantly fewer Graafian follicles in $Six3^{KissCre}$ mice. There was

no correlation between the number of Graafian follicles or corpora lutea in the infertile Six3^{KissCre} mice compared to the subfertile Six3^{KissCre} mice, suggesting the source of complete infertility is not driven by alterations in follicular development. While there is some Kiss1-Cre expression in the ovary (Ho et al., 2021), *Six3* is not detected in the adult ovary (Hsu et al., 2014), so we speculate that the reduction in Graafian follicles is driven by the loss of SIX3 in kisspeptin neurons. These phenotypes may be caused by disruption in sex steroid feedback, which is mediated by kisspeptin neurons and was disrupted on the morning of proestrus (Smith, 2008, 2013).

We also found that the increased cycle length in Six3^{KissCre} females was comparable to *Six3* heterozygous females, suggesting that SIX3 in kisspeptin neurons underlies this phenotype (Pandolfi et al., 2018). The infertile Six3^{KissCre} mice had more severe cycling impairments compared to the other Six3^{KissCre} mice, which may contribute to their inability to produce litters. Future studies of gonadotropin release would be needed to determine a more precise mechanism.

Successful ovulation is prompted by the circadian-gated LH surge that occurs on the evening of proestrus (de la Iglesia and Schwartz, 2006; Robertson et al., 2009). We found that Six3^{KissCre} females were able to generate an induced LH surge and that the loss of SIX3 did not alter *Kiss1* levels, *cFos* levels, or *Kiss1-cFos* colocalization at the time of the LH surge. Therefore, these mice can respond appropriately to the cues needed to induce ovulation in the presence of exogenous estrogen. Surprisingly, Six3^{KissCre} females had elevated LH serum levels in the morning of an E2-induced LH surge, when AVPV kisspeptin neuron activity and LH levels are expected to remain low (Marraudino et al., 2017; Wang et al., 2016). This finding suggests an impairment in negative feedback, which is regulated by ARC kisspeptin neurons. However, there were no detectable differences in ARC *Kiss1* mRNA on the morning of the induced LH surge, and diestrus female Six3^{KissCre} mice had normal circulating LH and FSH levels.

We next explored whether the cause of the elevated morning LH could be increased or mis-timed kisspeptin secretion from AVPV kisspeptin neurons. We found that AVPV *Kiss1* gene expression during the morning of the induced LH surge was not higher in Six3^{KissCre} mice. We observed a modest reduction in the percent of *Kiss1* cells colocalized with *cFos* in AM Six3^{KissCre} mice, but almost a doubling of *cFos* expression, leading us to postulate that SIX3 could indirectly mediate kisspeptin secretion through repression of *cFos* (Bullitt, 1990; Hoffman et al., 1993; Kovacs, 2008). In addition to being a marker of neuronal activity and immediate early gene (IEG), cFOS is a pleiotropic transcription factor that can form heterodimers with other IEGs to form the AP-1 transcription factor complex, which can then regulate gene expression (Coss et al., 2004; Karin et al., 1997). The murine *cFos* proximal promoter contains both a complete (−313 bp) and partial (−59 bp) SIX3 consensus sequence (Hoffmann et al., 2018) and we show here that SIX3 can act through either of these sites to repress *cFos*-Luc transcription in AVPV kisspeptin neurons *in vitro*. Other studies have indicated a role of cFOS as a potential regulator *Kiss1* gene expression, as *cFOS*-null mice have an 80% reduction in AVPV *Kiss1* mRNA per cell (Xie et al., 2015); however, a direct relationship between the two has not been established. We demonstrate that cFOS induces the m*Kiss1* promoter and can be suppressed by SIX3 overexpression *in vitro*. We postulate

that, in our model, the absence of SIX3 from the kisspeptin cells in the $Six3^{KissCre}$ mice drives the increase in *cFos* observed in the *Kiss1* neurons in the AM of the induced surge. While we do not observe a corresponding increase in *Kiss1 in vivo*, only 30% of *Kiss1* cells expressed *cFos* in the AM, which could make it difficult to detect *cFos*-induced changes in total *Kiss1* mRNA levels.

We found that SIX3 differentially regulates the human and mouse kisspeptin promoters *in vitro*, by acting as a repressor of hKiss-Luc transcription and having no effect on mKiss-Luc transcription in either ARC or AVPV kisspeptin cell lines. SIX3 is highly conserved with the amino acid sequence being identical between mouse and human (Kawakami et al., 2000), suggesting that the contrast is due to differences in the human and mouse promoters. SIX3 regulates transcription through binding of ATTA and ATTA-like motifs (Manavathi et al., 2007; Zhu et al., 2002). While both the human and mouse *KISS1/Kiss1* promoters contain several ATTA sites, the positions of the motifs are not conserved (http://genome.ucsc.edu/) (Kent et al., 2002).

Alternatively, the effects of SIX3 on *cFos* expression may be unrelated to increased LH levels, and SIX3 is instead directly regulating neuronal excitability. AVPV kisspeptin neurons integrate signals from the suprachiasmatic nucleus (SCN) to regulate the timing of the LH surge (Piet et al., 2015; Tonsfeldt et al., 2022). A recent study, which deleted *Six3* from mature neurons using Synapsin-Cre, revealed that SIX3 in mature neurons is important for proper alignment of circadian rhythms and fertility (Hoffmann et al., 2021). In the present study, we found that *Six3* expression in AVPV kisspeptin neurons is regulated by time of day and may be involved in gating of neuronal activity prior to the surge.

Overall, our study establishes the importance of kisspeptin-specific SIX3 in regulating estrous cycles and fertility in female mice, which contributes to the reproductive phenotype of Six3 heterozygous mice. We also propose that *Six3* is a novel regulator of *cFos*. Further, we demonstrate that *Six3* is regulated by time of day in AVPV kisspeptin neurons and may play a role in the circadian control of the LH surge, through repression of *cFos* within kisspeptin neurons.

Acknowledgements

We thank Alejandro Lomniczi and Sergio Ojeda for providing the hKiss-Luc plasmid, Steven Kliewer for providing the mKiss-Luc plasmid, and Patrick E. Chappell for providing the KTaR-1 and KTaV-3 cell lines. We thank Jessica Cassin for obtaining the single cell germ cell RNA expression data. We also thank Ichiko Saotome and Austin Chin for technical assistance and Daphne Bindels and the Nikon Imaging Core for developing the analysis pipeline to quantify our RNAscope images.

Funding

This work was supported by NIH grants R01 HD082567, R01 HD100580, and R01 HD072754 (to P.L.M.) and by P50 HD012303 as part of the National Centers for Translational Research in Reproduction and Infertility (P.L.M.). P.L.M. was partially supported by P30 DK063491, P42 ES010337, and P30 CA023100, all of which also supported the UCSD Transgenic Mouse and Embryonic Stem Cell Core. S.N. L. was partially supported by P42 ES010337, T32 GM008666, and a supplement to P50 HD012303. T.C. was partially supported by the Ledell Family Research Undergraduate Research Scholarship Award for Science and Engineering. J.H. was partially supported by The Endocrine Society Summer Research Fellowship Award, the BrightSpinnaker Fellowship Award, and the McNair Research Program. N.C.P.N. was partially supported by the McNair Research Program. M.Y.H. was partially supported by Doris A. Howell Research Scholarship for Women's Health and the Julia Brown Research Scholarship for Health and Medical Professions, or Medical Research. K.J.T. was partially supported by T32 HD007203,

F32 HD090837, and P42 ES010337. The University of Virginia Ligand Assay Core was supported by NIH P50 HD028934.

References

Atkin SD, Owen BM, Bookout AL, Cravo RM, Lee C, Elias CF, Elmquist JK, Kliewer SA, Mangelsdorf DJ, 2013. Nuclear receptor LRH-1 induces the reproductive neuropeptide kisspeptin in the hypothalamus. Mol. Endocrinol 27, 598–605. [PubMed: 23504956]

Au MG, Crowley WF Jr., Buck CL, 2011. Genetic counseling for isolated GnRH deficiency. Mol. Cell. Endocrinol 346, 102–109. [PubMed: 21664415]

Bianco SD, Kaiser UB, 2009. The genetic and molecular basis of idiopathic hypogonadotropic hypogonadism. Nat. Rev. Endocrinol 5, 569–576. [PubMed: 19707180]

Bullitt E, 1990. Expression of c-fos-like protein as a marker for neuronal activity following noxious stimulation in the rat. J. Comp. Neurol 296, 517–530. [PubMed: 2113539]

Byers SL, Wiles MV, Dunn SL, Taft RA, 2012. Mouse estrous cycle identification tool and images. PLoS One 7, e35538. [PubMed: 22514749]

Conte I, Morcillo J, Bovolenta P, 2005. Comparative analysis of Six 3 and Six 6 distribution in the developing and adult mouse brain. Dev. Dynam 234, 718–725.

Coss D, Jacobs SB, Bender CE, Mellon PL, 2004. A novel AP-1 site is critical for maximal induction of the follicle-stimulating hormone beta gene by gonadotropin-releasing hormone. J. Biol. Chem 279, 152–162. [PubMed: 14570911]

Cravo RM, Margatho LO, Osborne-Lawrence S, Donato J Jr., Atkin S, Bookout AL, Rovinsky S, Frazao R, Lee CE, Gautron L, Zigman JM, Elias CF, 2011. Characterization of Kiss1 neurons using transgenic mouse models. Neuroscience 173, 37–56. [PubMed: 21093546]

de la Iglesia HO, Schwartz WJ, 2006. Minireview: timely ovulation: circadian regulation of the female hypothalamo-pituitary-gonadal axis. Endocrinology 147, 1148–1153. [PubMed: 16373412]

Di Giorgio NP, Catalano PN, Lopez PV, Gonzalez B, Semaan SJ, Lopez GC, Kauffman AS, Rulli SB, Somoza GM, Bettler B, Libertun C, Lux-Lantos VA, 2013. Lack of functional GABAB receptors alters Kiss1 , Gnrh1 and Gad 1 mRNA expression in the medial basal hypothalamus at postnatal day 4. Neuroendocrinology 98, 212–223. [PubMed: 24080944]

Dror T, Franks J, Kauffman AS, 2013. Analysis of multiple positive feedback paradigms demonstrates a complete absence of LH surges and GnRH activation in mice lacking Kisspeptin signaling. Biol. Reprod 88, 146. [PubMed: 23595904]

Dungan HM, Gottsch ML, Zeng H, Gragerov A, Bergmann JE, Vassilatis DK, Clifton DK, Steiner RA, 2007. The role of kisspeptin-GPR54 signaling in the tonic regulation and surge release of gonadotropin-releasing hormone/luteinizing hormone. J. Neurosci 27, 12088–12095. [PubMed: 17978050]

Ely HA, Mellon PL, Coss D, 2011. GnRH induces the c-Fos gene via phosphorylation of SRF by the calcium/calmodulin kinase II pathway. Mol. Endocrinol 25, 669–680. [PubMed: 21292826]

Glidewell-Kenney CA, Shao PP, Iyer AK, Grove AM, Meadows JD, Mellon PL, 2013. Neurokinin B causes acute GnRH secretion and repression of GnRH transcription in GT1–7 GnRH neurons. Mol. Endocrinol 27, 437–454. [PubMed: 23393128]

Gottsch ML, Cunningham MJ, Smith JT, Popa SM, Acohido BV, Crowley WF, Seminara S, Clifton DK, Steiner RA, 2004. A role for kisspeptins in the regulation of gonadotropin secretion in the mouse. Endocrinology 145, 4073–4077. [PubMed: 15217982]

Herbison AE, 2018. The gonadotropin-releasing hormone pulse generator. Endocrinology 159, 3723–3736. [PubMed: 30272161]

Herbison AE, Porteous R, Pape JR, Mora JM, Hurst PR, 2008. Gonadotropin-releasing hormone (GnRH) neuron requirements for puberty, ovulation and fertility. Endocrinology 149, 597–604. [PubMed: 18006629]

Ho EV, Shi C, Cassin J, He MY, Nguyen RD, Ryan GE, Tonsfeldt KJ, Mellon PL, 2021. Reproductive deficits induced by prenatal antimullerian hormone exposure require androgen receptor in kisspeptin cells. Endocrinology 162, bqab197. [PubMed: 34529765]

Hoffman GE, Smith MS, Verbalis JG, 1993. c-Fos and related immediate early gene products as markers of activity in neuroendocrine systems. Front. Neuroendocrinol 14, 173–213. [PubMed: 8349003]

Hoffmann HM, 2018. Determination of reproductive competence by confirming pubertal onset and performing a fertility assay in mice and rats. JoVE, e58352.

Hoffmann HM, Gong P, Tamrazian A, Mellon PL, 2018. Transcriptional interaction between cFOS and the homeodomain-binding transcription factor VAX1 on the GnRH promoter controls Gnrh1 expression levels in a GnRH neuron maturation specific manner. Mol. Cell. Endocrinol 461, 143–154. [PubMed: 28890143]

Hoffmann HM, Meadows JD, Breuer JA, Yaw AM, Nguyen D, Tonsfeldt KJ, Chin AY, Devries BM, Trang C, Oosterhouse HJ, Lee JS, Doser JW, Gorman MR, Welsh DK, Mellon PL, 2021. The transcription factors SIX3 and VAX1 are required for suprachiasmatic nucleus circadian output and fertility in female mice. J. Neurosci. Res 99, 2625–2645. [PubMed: 34212416]

Hoffmann HM, Pandolfi EC, Larder R, Mellon PL, 2019. Haploinsufficiency of homeodomain proteins Six3, Vax1, and Otx2 causes subfertility in mice via distinct mechanisms. Neuroendocrinology 109, 200–207. [PubMed: 30261489]

Hoffmann HM, Tamrazian A, Xie H, Perez-Millan MI, Kauffman AS, Mellon PL, 2014. Heterozygous deletion of ventral anterior homeobox (vax1) causes subfertility in mice. Endocrinology 155, 4043–4053. [PubMed: 25060364]

Hoffmann HM, Trang C, Gong P, Kimura I, Pandolfi EC, Mellon PL, 2016. Deletion of Vax1 from gonadotropin-releasing hormone (GnRH) neurons abolishes GnRH rxpression and leads to hypogonadism and infertility. J. Neurosci 36, 3506–3518. [PubMed: 27013679]

Hsu MC, Wang JY, Lee YJ, Jong DS, Tsui KH, Chiu CH, 2014. Kisspeptin modulates fertilization capacity of mouse spermatozoa. Reproduction 147, 835–845. [PubMed: 24567427]

Jacobs DC, Veitch RE, Chappell PE, 2016. Evaluation of immortalized AVPV- and Arcuate-specific neuronal kisspeptin cell lines to elucidate potential mechanisms of estrogen responsiveness and temporal cene expression in females. Endocrinology 157, 3410–3419. [PubMed: 27409645]

Karin M, Liu Z, Zandi E, 1997. AP-1 function and regulation. Curr. Opin. Cell Biol 9, 240–246. [PubMed: 9069263]

Kauffman AS, 2010. Coming of age in the kisspeptin era: sex differences, development, and puberty. Mol. Cell. Endocrinol 324, 51–63. [PubMed: 20083160]

Kawakami K, Sato S, Ozaki H, Ikeda K, 2000. Six family genes–structure and function as transcription factors and their roles in development. Bioessays 22, 616–626. [PubMed: 10878574]

Kent WJ, Sugnet CW, Furey TS, Roskin KM, Pringle TH, Zahler AM, Haussler D, 2002. The human genome browser at UCSC. Genome Res. 12, 996–1006. [PubMed: 12045153]

Kovacs KJ, 2008. Measurement of immediate-early gene activation- c-fos and beyond. J. Neuroendocrinol 20, 665–672. [PubMed: 18601687]

Lagutin OV, Zhu CC, Kobayashi D, Topczewski J, Shimamura K, Puelles L, Russell HR, McKinnon PJ, Solnica-Krezel L, Oliver G, 2003. Six3 repression of Wnt signaling in the anterior neuroectoderm is essential for vertebrate forebrain development. Genes Dev. 17, 368–379. [PubMed: 12569128]

Lavalle SN, Hoffmann HM, Chou T, Hernandez J, Naing NCP, Tonsfeldt KJ, Mellon PL, 2021. Kiss1 is differentially regulated in male and female mice by the homeodomain transcription factor VAX1. Mol. Cell. Endocrinol 534, 111358. [PubMed: 34098016]

Liu W, Lagutin OV, Mende M, Streit A, Oliver G, 2006. Six3 activation of Pax 6 expression is essential for mammalian lens induction and specification. EMBO J. 25, 5383–5395. [PubMed: 17066077]

Madisen L, Zwingman TA, Sunkin SM, Oh SW, Zariwala HA, Gu H, Ng LL, Palmiter RD, Hawrylycz MJ, Jones AR, Lein ES, Zeng H, 2010. A robust and high-throughput Cre reporting and characterization system for the whole mouse brain. Nat. Neurosci 13, 133–140. [PubMed: 20023653]

Manavathi B, Peng S, Rayala SK, Talukder AH, Wang MH, Wang RA, Balasenthil S, Agarwal N, Frishman LJ, Kumar R, 2007. Repression of Six3 by a corepressor regulates rhodopsin expression. Proc. Natl. Acad. Sci. U. S. A 104, 13128–13133. [PubMed: 17666527]

Marraudino M, Miceli D, Farinetti A, Ponti G, Panzica G, Gotti S, 2017. Kisspeptin innervation of the hypothalamic paraventricular nucleus: sexual dimorphism and effect of estrous cycle in female mice. J. Anat 230, 775–786. [PubMed: 28295274]

McQuillan HJ, Han SY, Cheong I, Herbison AE, 2019. GnRH pulse generator activity across the estrous cycle of female mice. Endocrinology 160, 1480–1491. [PubMed: 31083714]

Messager S, Chatzidaki EE, Ma D, Hendrick AG, Zahn D, Dixon J, Thresher RR, Malinge I, Lomet D, Carlton MB, Colledge WH, Caraty A, Aparicio SA, 2005. Kisspeptin directly stimulates gonadotropin-releasing hormone release via G protein-coupled receptor 54. Proc. Natl. Acad. Sci. U.S.A 102, 1761–1766. [PubMed: 15665093]

Mueller JK, Dietzel A, Lomniczi A, Loche A, Tefs K, Kiess W, Danne T, Ojeda SR, Heger S, 2011. Transcriptional regulation of the human KiSS1 gene. Mol. Cell. Endocrinol 342, 8–19. [PubMed: 21672609]

Pandolfi EC, Hoffmann HM, Schoeller EL, Gorman MR, Mellon PL, 2018. Haploinsufficiency of SIX3 abolishes male reproductive behavior rhrough disrupted olfactory development, and impairs female fertility through disrupted GnRH neuron migration. Mol. Neurobiol 55, 8709–8727. [PubMed: 29589282]

Piet R, Fraissenon A, Boehm U, Herbison AE, 2015. Estrogen permits vasopressin signaling in preoptic kisspeptin neurons in the female mouse. J. Neurosci 35, 6881–6892. [PubMed: 25926463]

Robertson JL, Clifton DK, de la Iglesia HO, Steiner RA, Kauffman AS, 2009. Circadian regulation of Kiss1 neurons: implications for timing the preovulatory gonadotropin-releasing hormone/luteinizing hormone surge. Endocrinology 150, 3664–3671. [PubMed: 19443569]

Smith JT, 2008. Kisspeptin signalling in the brain: steroid regulation in the rodent and Ewe. Brain Res. Rev 57, 288–298. [PubMed: 17509691]

Smith JT, 2013. Sex steroid regulation of kisspeptin circuits. Adv. Exp. Med. Biol 784, 275–295. [PubMed: 23550011]

Smith JT, Cunningham MJ, Rissman EF, Clifton DK, Steiner RA, 2005a. Regulation of Kiss1 gene expression in the brain of the female mouse. Endocrinology 146, 3686–3692. [PubMed: 15919741]

Smith JT, Dungan HM, Stoll EA, Gottsch ML, Braun RE, Eacker SM, Clifton DK, Steiner RA, 2005b. Differential regulation of KiSS-1 mRNA expression by sex steroids in the brain of the male mouse. Endocrinology 146, 2976–2984. [PubMed: 15831567]

Smith JT, Popa SM, Clifton DK, Hoffman GE, Steiner RA, 2006. Kiss1 neurons in the forebrain as central processors for generating the preovulatory luteinizing hormone surge. J. Neurosci 26, 6687–6694. [PubMed: 16793876]

Stephens SB, Tolson KP, Rouse ML Jr., Poling MC, Hashimoto-Partyka MK, Mellon PL, Kauffman AS, 2015. Absent progesterone signaling in kisspeptin neurons disrupts the LH surge and impairs fertility in female mice. Endocrinology 156, 3091–3097. [PubMed: 26076042]

Sunnen CN, Simonet JC, Marsh ED, Golden JA, 2014. Arx is required for specification of the zona incerta and reticular nucleus of the thalamus. J. Neuropathol. Exp. Neurol 73, 253–261. [PubMed: 24487799]

Tonsfeldt KJ, Mellon PL, Hoffmann HM, 2022. Circadian rhythms in the neuronal network timing the luteinizing hormone surge. Endocrinology 163 (2), 1–10 bqab268.

Tonsfeldt KJ, Schoeller EL, Brusman LE, Cui LJ, Lee J, Mellon PL, 2019. The contribution of the dircadian gene Bmal1 to female fertility and the generation of the preovulatory Luteinizing Hormone surge. J Endocr Soc 3, 716–733. [PubMed: 30906911]

Topaloglu AK, 2017. Update on the genetics of idiopathic hypogonadotropic hypogonadism. J Clin Res Pediatr Endocrinol 9, 113–122. [PubMed: 29280744]

Wang L, DeFazio RA, Moenter SM, 2016. Excitability and burst generation of AVPV kisspeptin neurons are regulated by the estrous cycle via multiple conductances modulated by estradiol action. eNeuro 3. ENEURO.0094–0016.2016.

Xie C, Jonak CR, Kauffman AS, Coss D, 2015. Gonadotropin and kisspeptin gene expression, but not GnRH, are impaired in cFOS deficient mice. Mol. Cell. Endocrinol 411, 223–231. [PubMed: 25958044]

Zhu CC, Dyer MA, Uchikawa M, Kondoh H, Lagutin OV, Oliver G, 2002. Six3-mediated auto repression and eye development requires its interaction with members of the Groucho-related family of co-repressors. Development 129, 2835–2849. [PubMed: 12050133]

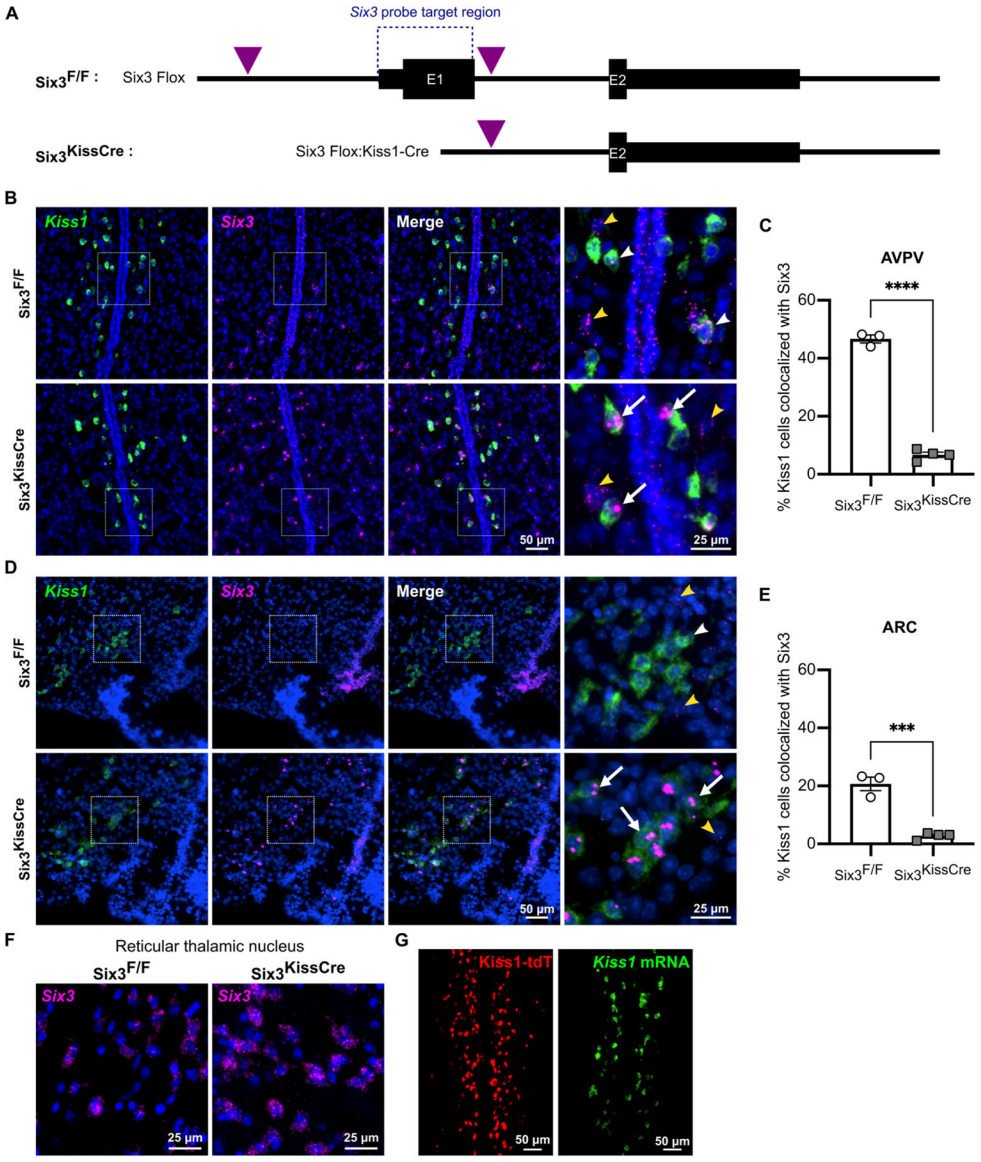

Fig. 1.

Six3 is expressed in AVPV and ARC kisspeptin neurons in mice. A) Schematic of the *Six3* gene in kisspeptin cells in $Six3^{Flox/Flox}$ ($Six3^{F/F}$) and $Six3^{KissCre}$ mice. Triangles represent LoxP sites. Exon 1 (E1) and exon 2 (E2) are represented by the larger black rectangles. Dotted line indicates the region targeted by the *Six3* probe. Representative images of fluorescent *in situ* hybridization to detect *Kiss1* (green) and *Six3* (magenta) in the B) AVPV of OVX + E2 treated and D) ARC of OVX females. Sections were counterstained with DAPI (blue) to visual nuclei. White arrowheads depict examples of *Six3* and *Kiss1* colocalization, yellow arrowheads depict *Six3* expression in *Kiss1*-negative cells, and white arrows depict atypical *Six3* signal in *Kiss1*-positive cells. Quantification of the percent of *Six3* colocalized with *Kiss1* in the C) AVPV and E) ARC. Data were analyzed by Student's t-test. Significance indicated by ***$p < 0.0005$, ****$p < 0.0001$. N = 3–4. F) Fluorescent images of *Six3* (magenta) *in situ* hybridization in the reticular

thalamic nucleus of $Six3^{Flox/Flox}$ and $Six3^{KissCre}$ OVX females. G) Fluorescent images of tdTomato (red) immunostaining and *Kiss1* (green) *in situ* hybridization in the AVPV of intact $Kiss1^{Cre}$:tdTomato and OVX + E2 $Six3^{Flox/Flox}$ females, respectively.

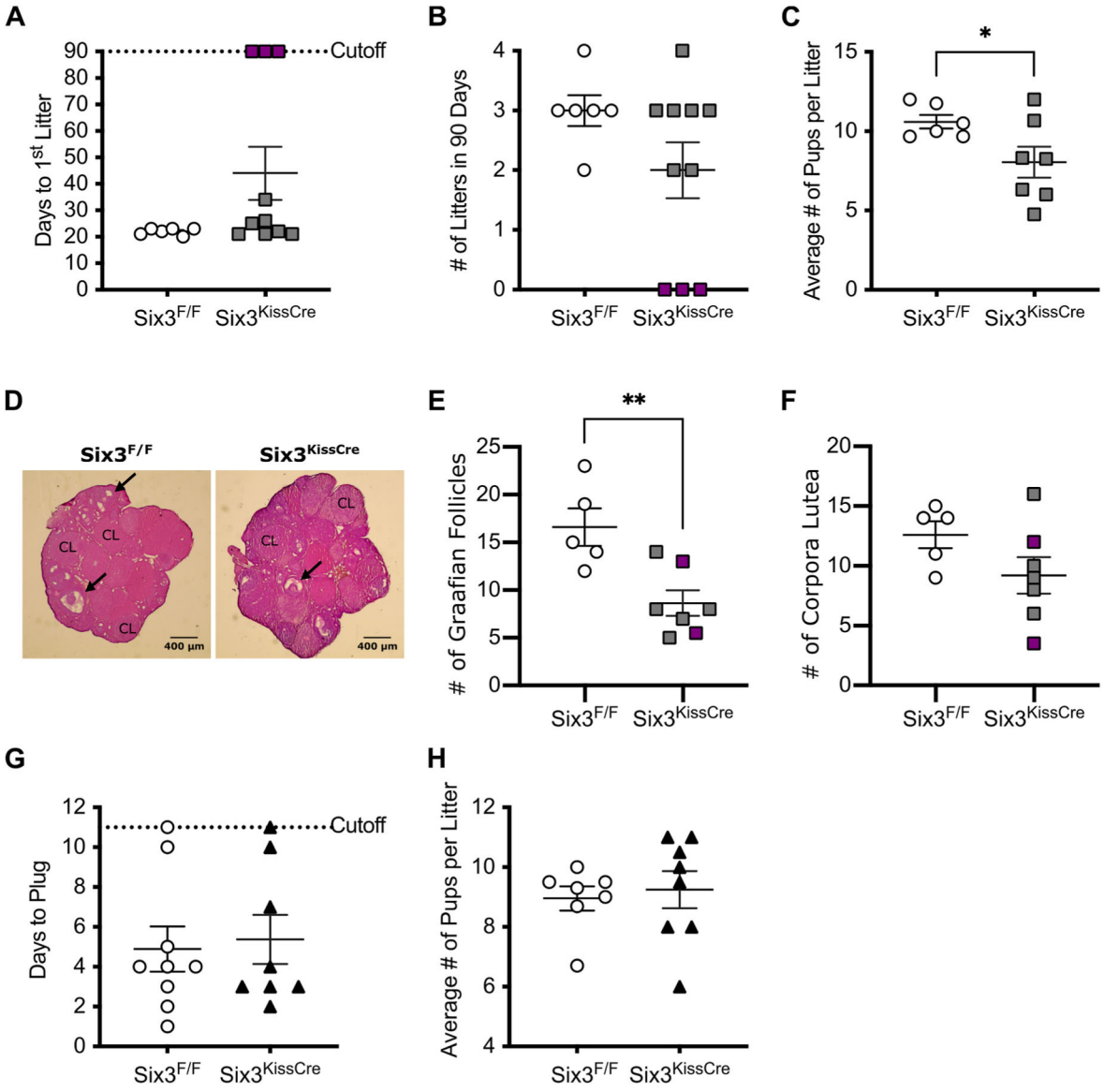

Fig. 2.

Six3 within kisspeptin cells is necessary for female fecundity. A) Number of days between pairing and first litter in $Six3^{F/F}$ and $Six3^{KissCre}$ female mice. Dotted line indicates a 90-day cutoff. B) Number of litters produced in 90 days by female mice. C) Average number of pups born per litter in female mice. D) Representative images of ovaries from $Six3^{F/F}$ and $Six3^{KissCre}$ females collected after fertility assay. Arrows depict examples of Graafian follicles, CL depicts examples of corpora lutea. E) Quantification of the number of Graafian follicles per ovary. F) Quantification of the number of corpora lutea per ovary. G) Number of days for $Six3^{F/F}$ and $Six3^{KissCre}$ males to plug wildtype females. H) Average number of pups produced per litter by wildtype females when paired with male $Six3^{F/F}$ or $Six3^{KissCre}$ mice. All data were analyzed by Student's t-test or Welch's *t*-test. N = 5–10. Significance indicated by * $p < 0.05$, ** $p < 0.005$. Purple squares represent the infertile $Six3^{KissCre}$ female mice.

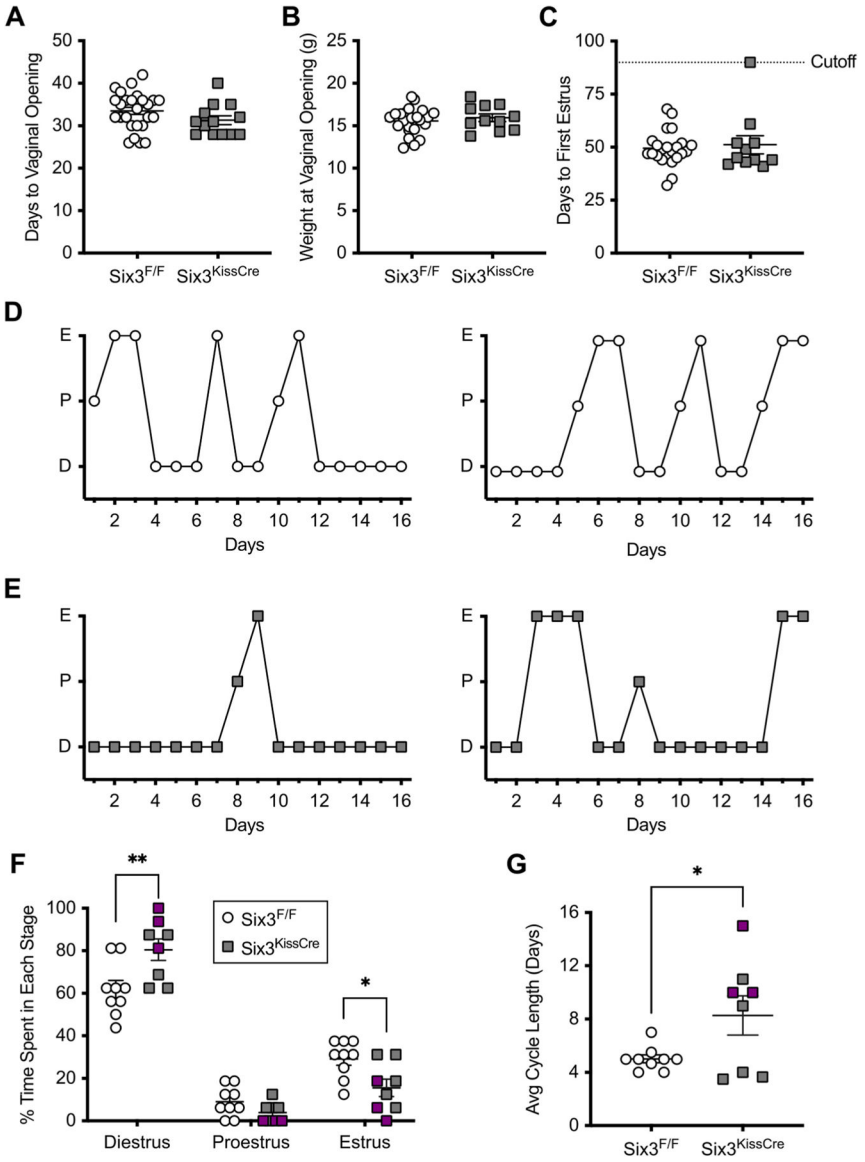

Fig. 3.

Loss of *Six3* from kisspeptin neurons disrupts estrous cyclicity. A) Time to pubertal onset determined by vaginal opening. N = 13–26. B) Weight of mice the day of vaginal opening. N = 13–26. C) Time to first estrus stage. N = 11–22. Representative cycles from: D) two $Six3^{F/F}$ females and E) two $Six3^{KissCre}$ females. D indicates diestrus, P indicates proestrus, and E indicates estrus. F) Percent of time spent in each stage of the estrous cycle. White circles represent $Six3^{F/F}$ mice and grey squares represent $Six3^{KissCre}$ mice. N = 8–9. G) Average time to complete one estrous cycle, measured from diestrus to diestrus. N = 8–9. Data were analyzed by two-way ANOVA or Student's t-test. Significance is indicated by: *p < 0.05, **p < 0.005. Purple squares represent the infertile $Six3^{KissCre}$ female mice.

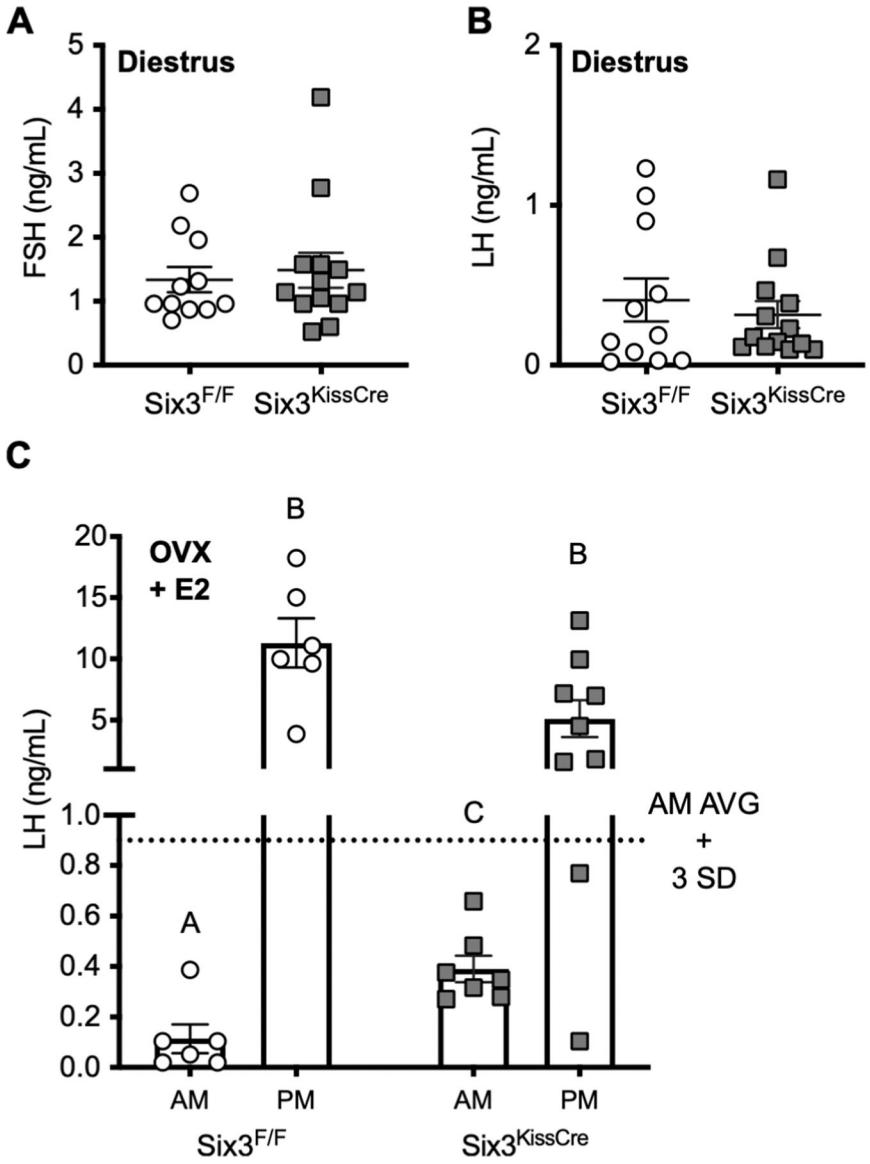

Fig. 4.

Serum gonadotropins in female mice. Circulating serum levels of A) FSH and B) LH in diestrus-staged female mice collected between ZT 4–6. Data were analyzed by Student's t-test. N = 11–13. C) Serum LH levels in OVX + E2 treated mice collected at ZT 4–5 (AM) or ZT 12–13 (PM). Dotted line indicates surge threshold (combined AM average + 3 SD = 0.9 ng/mL). Data were log transformed prior to analysis by two-way ANOVA. N = 5–7. Significance of $p < 0.05$ indicated by different letters.

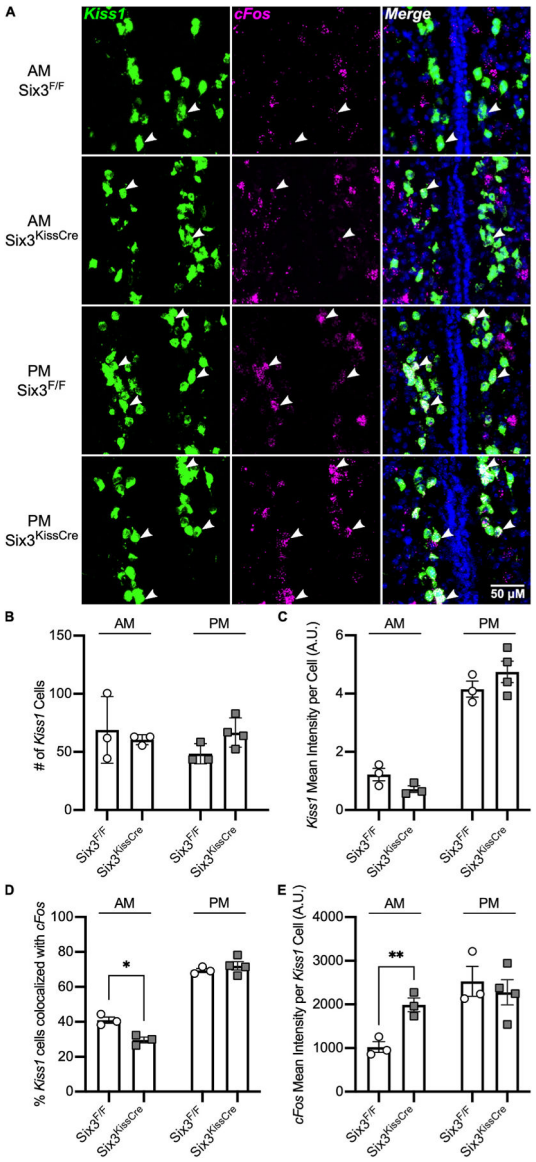

Fig. 5.

The loss of SIX3 from kisspeptin neurons reduces the percent of *Kiss1* cells colocalized with *cFos*. A) Representative images of fluorescent *in situ* hybridization to detect *Kiss1* (green), *cFos* (magenta) in the AVPV of OVX + E2 treated females collected at ZT 4–5 (AM) or ZT 12–13 (PM). *Kiss1* and *cFos* colocalization are visualized in white. Arrows depict examples of *Kiss1-cFos* colocalization. Sections were counterstained with DAPI (blue) for visualization of the nuclei. B) The number of *Kiss1* expressing cells. C) Mean intensity of *Kiss1* in arbitrary units (A.U.). D) Percent of *Kiss1*-cells colocalized with *cFos*. E) Mean intensity of *cFos* within *Kiss1*-positive cells. Student's t-test between indicated pairs. N = 3–4. Significance indicated by * $p < 0.05$ and **$p < 0.05$.

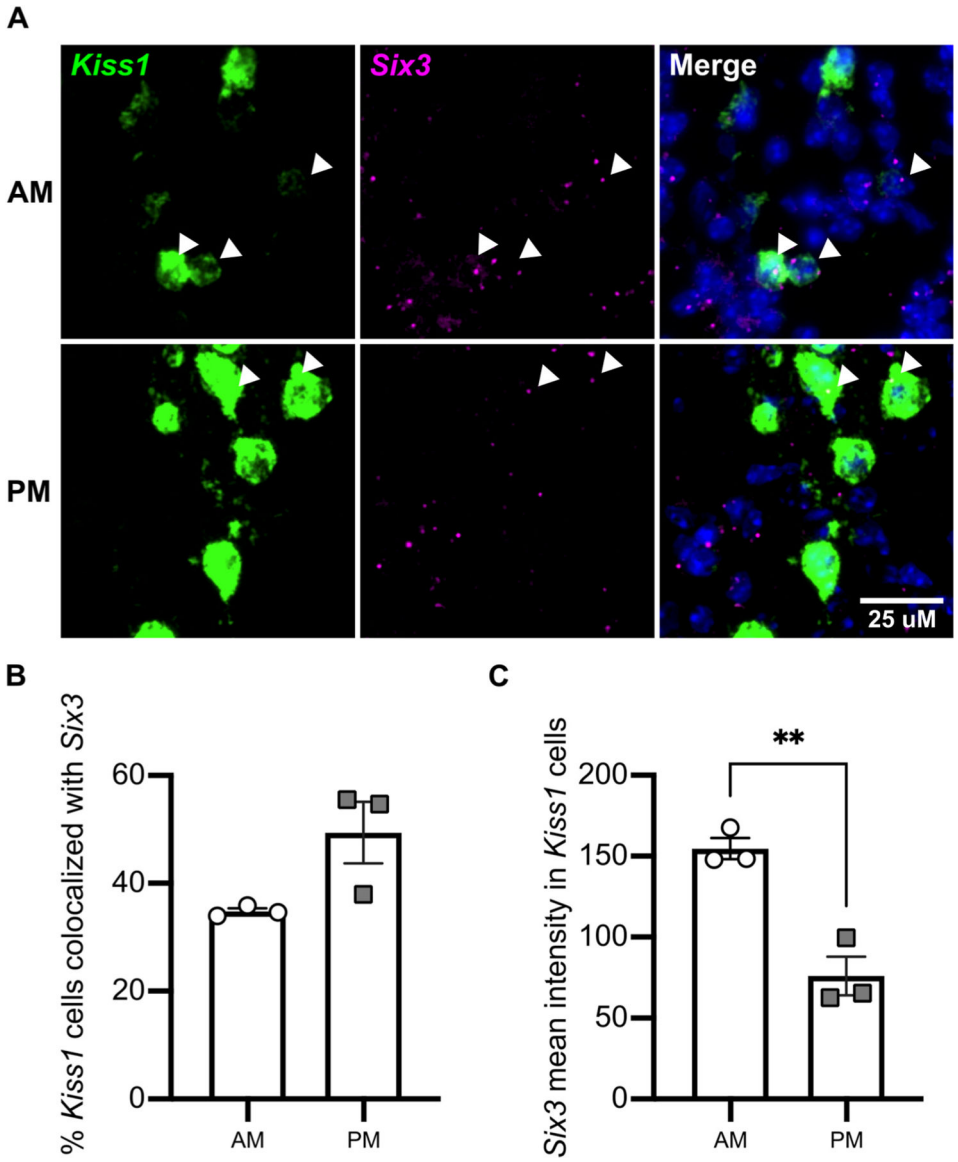

Fig. 6. *Six3* intensity is regulated by time of day in OVX + E2-treated Six3 WT mice.

A) Representative images of fluorescent *in situ* hybridization to detect *Kiss1* (green) and *Six3* (magenta) in the AVPV of OVX + E2 treated females collected at ZT 4–5 (AM) or ZT 12–13 (PM). Sections were counterstained with DAPI (blue) to visual nuclei. White triangles depict examples of *Kiss1* and *Six3* colocalization. B) Quantification of the percent of *Kiss1* cells colocalized with *Six3*. (C) Quantification of *Six3* mean intensity within *Kiss1*-positive cells. Data were analyzed by student's t-test. N = 3. Significance indicated by **$p < 0.05$.

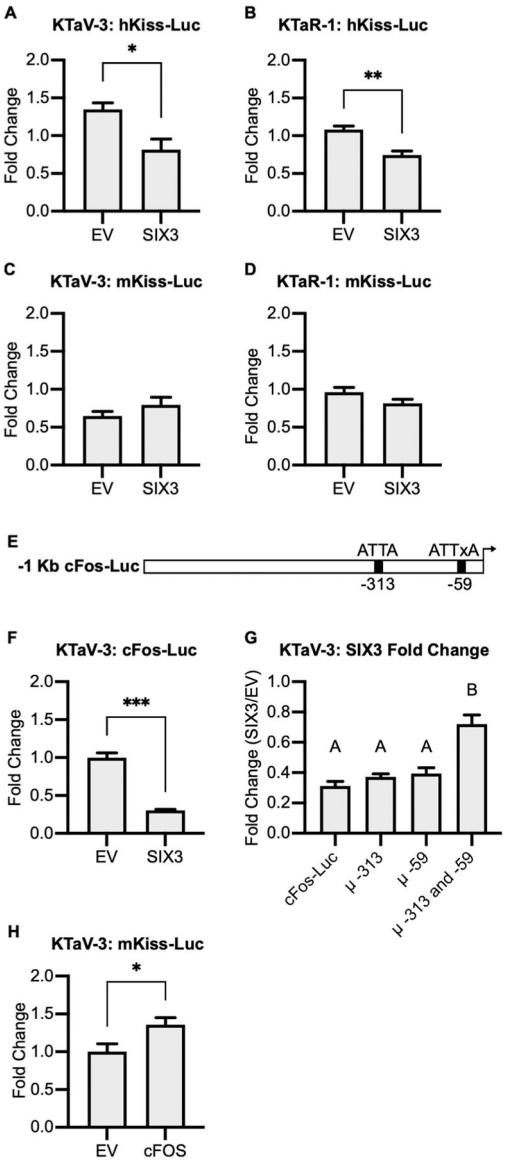

Fig. 7. SIX3 represses cFos-Luc transcription *in vitro*.

hKiss-Luc was cotransfected with 20 ng SIX3 or empty vector (EV) in A) KTaV-3 and B) KTaR-1 cells. mKiss-Luc was co-transfected with 20 ng SIX3 or EV in C) KTaV-3 and D) KTaR-1 cells. E) Schematic of SIX3 binding sites on the murine −1 Kb cFos promoter. F) cFos-Luc was co-transfected into KTaV-3 cells with 20 ng SIX3 or EV. G) cFos-Luc or cFos-luc reporters containing *cis*-mutations at −313 (μ −313), −59 (μ −59), or both (μ −313 and −59) base pairs were co-transfected with 20 ng SIX3 or EV. Data are represented as fold change of SIX3/EV. H) mKiss-luc was co-transfected into KTaV-3 cells with 50 ng cFOS or EV. For all experiments, bars represent means ± SEM, N = 3–5. Data were analyzed using Student's t-test or One-way ANOVA. Significance indicated by * $p < 0.05$, ** $p < 0.005$, *** $p < 0.0005$, or different letters $p < 0.05$.